IL NUOVO CIMENTO **38 C** (2015) 152
DOI 10.1393/ncc/i2015-15152-8

COLLOQUIA: LaThuile15

CMS supersymmetry and exotic Higgs results

R. YOHAY on behalf of the CMS COLLABORATION
Department of Physics, University of California, Davis - Davis, California, USA

received 2 October 2015

Summary. — A selection of results covering searches for supersymmetric particles and exotic decays of the Higgs boson are presented. These results are based on 8 TeV proton-proton collision data collected by the Compact Muon Solenoid experiment at the Large Hadron Collider.

PACS 11.30.Pb – Supersymmetry.
PACS 14.80.Da – Supersymmetric Higgs bosons.
PACS 14.80.Bn – Standard-model Higgs bosons.

1. – Introduction

Supersymmetry (SUSY) [1] offers a clear and elegant solution to the hierarchy problem. To date, there have only been null results in searches for SUSY at the Large Hadron Collider (LHC) and elsewhere, but there are still many reasons to continue looking. Searches targeting third generation sfermions can yield important insights into naturalness, yet because of large $t\bar{t}$ backgrounds and the difficulties of b and tau tagging, there is still a lot of unexplored parameter space in this area. Many early SUSY searches at the LHC have focused on the minimal SUSY standard model (MSSM) with gravity-mediated breaking, but there are lots of models that extend the MSSM that have not yet been fully addressed experimentally. Finally, the discovery of the 125 GeV Standard Model (SM) Higgs boson [2, 3] gives new impetus to searches targeting the SUSY Higgs sector.

In these proceedings, new results from data collected by the Compact Muon Solenoid (CMS) experiment during the 2012 8 TeV run of the LHC are presented. CMS is a general purpose detector composed of an inner silicon vertexing and tracking system, a total absorption crystal electromagnetic calorimeter, a brass/scintillator sampling hadronic calorimeter, and gaseous muon detectors. The solenoid provides a 3.8 T magnetic field that affords good charged particle momentum resolution and charge identification. Overall, the detector has a very high efficiency for electrons, muons, and photons and exploits a novel particle flow tau and jet reconstruction.

More details about the CMS detector can be found in ref. [4]. These results broadly cover the areas of SUSY and exotic Higgs decays, as well as showcase the range of data analysis techniques employed in the search for physics beyond the Standard Model at CMS.

2. – Searches for gravity-mediated SUSY

2˙1. *All-hadronic final states with the M_{T2} discriminator.* – Two key predictions of R-parity conserving SUSY are that (1) squarks and gluinos will be produced in pairs at colliders, and (2) in gravity-mediated models, the next-to-lightest sparticle will decay to a lightest neutralino (LSP) that is stable and leaves a signature of missing momentum in a 4π detector [1]. The M_{T2} discriminator [5] was developed to characterize the transverse component of missing momentum p_T^{miss} in events with two heavy squarks or gluinos that each decay to quarks and an LSP. QCD di-jet events, even those with significant observed p_T^{miss} due to jet mis-measurement, tend to have low values of M_{T2}, while SUSY events with multiple jets and true p_T^{miss} (the latter due to the escaping LSP) tend to have high values of M_{T2}. Cutting on M_{T2} renders the di-jet background insignificant, leaving only backgrounds with true p_T^{miss} (W, $t\bar{t}$, and $Z \to \nu\nu$) and QCD multi-jet production.

The analysis combines 123 signal regions defined by light (u, d, c, and s quark and gluon) jet multiplicity, b jet multiplicity, p_T^{miss}, the scalar sum H_T of the transverse momenta of all jets in the event with $p_T > 50$ GeV and $|\eta| < 3$, and M_{T2}. The three triggers require either $H_T > 650$ GeV, $|p_T^{miss}| > 150\,\text{GeV}$, or $H_T > 350\,\text{GeV}$ and $|p_T^{miss}| > 100\,\text{GeV}$. Jets are reconstructed with the anti-k_T algorithm with $R = 0.5$, and are corrected both for nonuniform response over p_T and η and the effect of overlapping particles from secondary pp collisions (pileup). b jets are required to have $p_T > 40\,\text{GeV}$ and pass a cut on the Combined Secondary Vertex (CSV) discriminator, which identifies them based on the b lifetime. Events are required to contain at least two jets with $p_T > 100\,\text{GeV}$ and $|\eta| < 2.4$, zero leptons (to reduce the background from W, Z, and $t\bar{t}$), and to satisfy a number of noise cleaning cuts. Additional cuts on the angles between jets and p_T^{miss} help reduce the QCD multi-jet background. The trigger is $> 99\%$ efficient for events selected this way. For more details on the analysis methods, including the veto lepton definition, and references to CMS reconstruction techniques, see ref. [6].

$Z \to \nu\nu+$ jets constitutes the main background for categories with lower numbers of jets and is estimated from photon + jet events, with the photon momentum treated as p_T^{miss}, scaled by the theoretical cross-section ratio of $Z \to \nu\nu$ + jets to photon + jets. At higher jet multiplicity, the background from W and $t\bar{t}$ events where one lepton fails the veto dominates. It is estimated from data control samples requiring, rather than vetoing, one lepton, and is normalized by a factor depending on the lepton identification efficiency.

2˙2. *b-tagged events using the razor discriminants.* – The razor discriminants M_R and R [7], like M_{T2}, effectively remove the QCD background from a jets $+p_T^{miss}$ search, while simultaneously characterizing the mass scale of new physics if it exists. They are therefore well suited to a broad search for evidence of stops in exclusive categories defined by the number of leptons, light jets, and b jets. In the CMS razor analysis with b tags [8], all events are required to contain at least one b jet and satisfy a loose requirement on M_R and R at the trigger level. In each category, a background-dominated sideband in the R^2-M_R plane is then fit with an empirical function and extrapolated to the signal region. No significant excess is observed in any of the categories, so LHC-style CL_S limits are set on an array of simplified models involving gluino or stop pair production. The SUSY signal shapes as a function of (R^2, M_R) are considered in the limit.

2˙3. *Combination of searches for SUSY events with 4 W bosons.* – The results of a combination of five CMS analyses are presented as limits on (1) gluino pair production

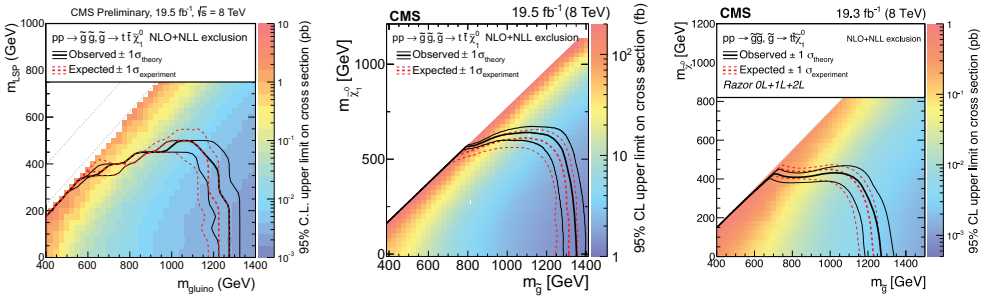

Fig. 1. – Comparison between the M_{T2} (left), 4-W (middle), and razor (right) analyses in exclusion reach in the m_{LSP}-$m_{\tilde{g}}$ plane for a simplified model of gluino pair production and decay to two tops and an LSP.

and decay to four top quarks and two LSPs or (2) sbottom pair production and decay to two top quarks, two W bosons, and two LSPs. The five analyses cover different final states: fully hadronic, single-lepton, same-sign di-lepton, opposite-sign di-lepton, and multi-lepton. References to all participating analyses can be found in ref. [9].

A comparison between the M_{T2}, 4-W, and razor analyses in exclusion reach in the m_{LSP}-$m_{\tilde{g}}$ plane is shown in fig. 1 for a simplified model of gluino pair production and decay to two tops and an LSP. Here, the 4-W combination provides the best sensitivity due to the large number of channels and direct targeting of the four-top final state. For direct stop production, the M_{T2} and razor analyses can be compared as in fig. 2. The expected reach of the two analyses is similar, although due to a downward fluctuation in one of the M_{T2} control samples, the actual reach is larger in the razor analysis.

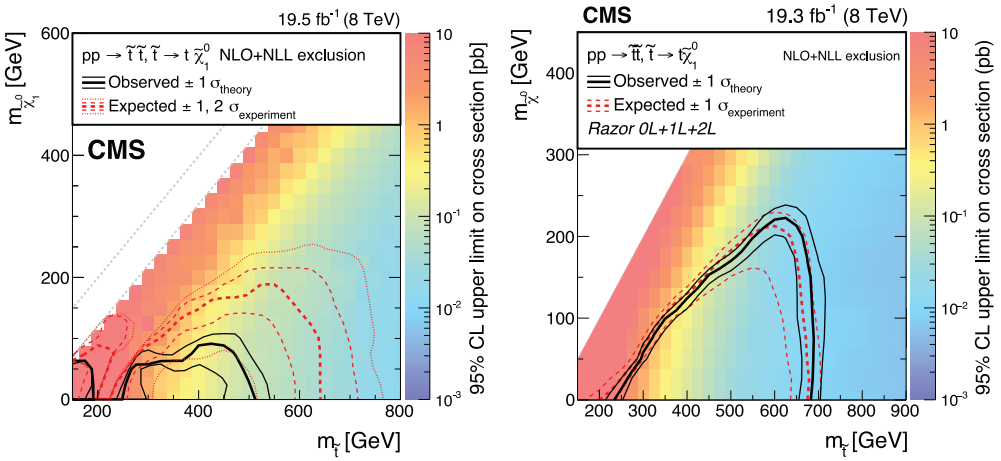

Fig. 2. – Comparison between the M_{T2} (left) and razor (right) analyses in exclusion reach in the m_{LSP}-$m_{\tilde{t}}$ plane for a simplified model of stop pair production and decay to a top and an LSP.

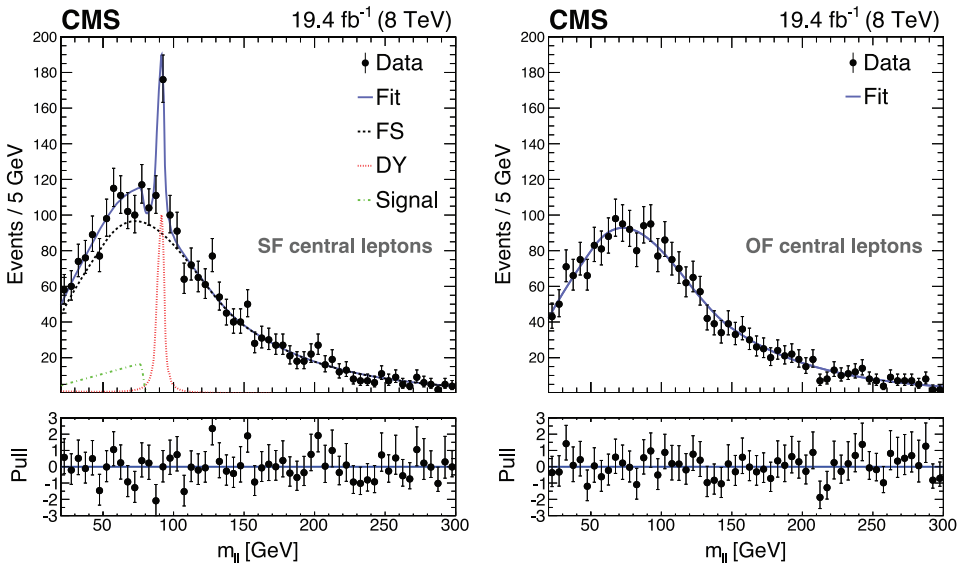

Fig. 3. – Fits to signal region (left) and opposite-flavor control region (right) data in the opposite-sign di-leptons analysis. More details about the fit can be found in ref. [11].

2˙4. *Opposite-sign lepton pairs, jets, and missing momentum.* – In addition to the classic multi-jet signature of R-parity-conserving SUSY, final states with multiple leptons and $p_{\mathrm{T}}^{\mathrm{miss}}$ are also possible. Cascade decays via a slepton can result in a pair of opposite-sign leptons and the LSP, where the di-lepton invariant mass spectrum exhibits an edge [10] at the value of the slepton mass. There are also decays via an off-shell Z to an opposite-sign di-lepton pair that do not exhibit such an edge. In both cases, there are accompanying jets due to the cascade decay of the pair-produced squarks or gluinos.

The CMS opposite-sign di-lepton analysis [11] requires a pair of isolated opposite-sign electrons or muons with $p_{\mathrm{T}} > 20$ GeV and $|\eta| < 2.4$, although these proceedings focus on the central region $|\eta| < 1.4$. Events are classified into signal regions according to $p_{\mathrm{T}}^{\mathrm{miss}}$ and the number of jets with $p_{\mathrm{T}} > 40$ GeV and $|\eta| < 3.0$ in the event. The main backgrounds are Drell-Yan di-lepton production and $t\bar{t}$ with opposite-sign, same-flavor leptons. The former is independently estimated from two data control regions: photon + jet events, which are weighted to accurately describe the hadronic activity in Drell-Yan events; and Z + jet events in which the jet-Z balance (JZB) [12] is negative (signal events are required to have positive JZB). The latter is estimated from an opposite-sign, opposite-flavor control sample. A fit describing the two background components and signal component is performed to the di-lepton invariant mass distribution to try to extract an edge position in the case of an excess. An excess with local significance 2.4σ is seen at the best-fit edge position of 78.7 ± 1.4 GeV, as shown in fig. 3.

The results are translated into upper limits on simplified SUSY models of sbottom pair production with $\tilde{b} \to \tilde{\chi}_2^0 b$. In fig. 4 (left), one of the $\tilde{\chi}_2^0$s decays via a slepton with mass 70 GeV to $l^+l^-\tilde{\chi}_1^0$. In fig. 4 (right), the $\tilde{\chi}_2^0$s decays via an off-shell Z to an LSP with mass 100 GeV. The observed limit in fig. 4 (left) is worse than the expected because of the small excess observed.

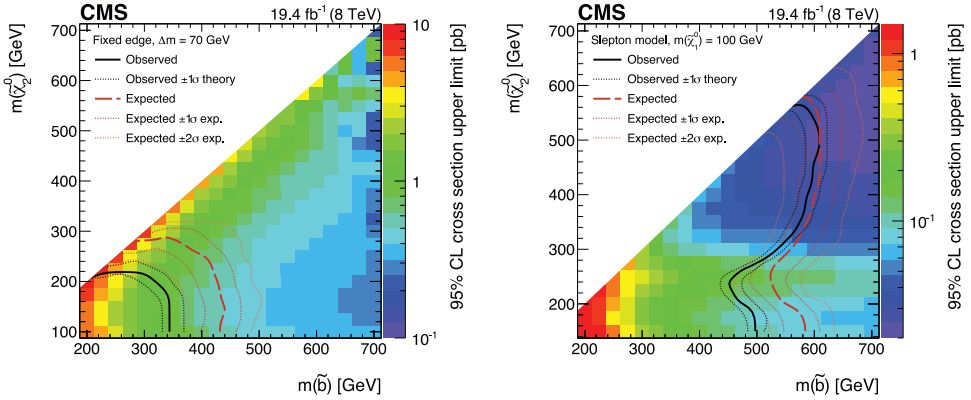

Fig. 4. – Limit curves in the $m_{\tilde{\chi}_2^0}$-$m_{\tilde{b}}$ plane for SUSY simplified models derived from the opposite-sign di-leptons search. Left: $\tilde{\chi}_2^0 \to l^+l^-\tilde{\chi}_1^0$ via slepton, $m_{\tilde{l}} = 70\,\text{GeV}$. Right: $\tilde{\chi}_2^0 \to l^+l^-\tilde{\chi}_1^0$ via Z^*, $m_{\tilde{\chi}_1^0} = 100\,\text{GeV}$.

3. – Searches for exotic Higgs decays

3˙1. *Lepton-flavor-violating Higgs.* – Many models of physics beyond the Standard Model generically predict lepton flavor violation (for a list, see ref. [13]). The CMS results presented here come from the first direct search for lepton flavor violation in the decays of the recently discovered Higgs boson. Six channels are combined: $\mu\tau_\text{h}$, where τ_h refers to a hadronic tau decay ($\times 3$ jet bins); and $\mu\tau_e$, where τ_e refers to a tau decay to an electron ($\times 3$ jet bins). In the $\mu\tau_\text{h}$ channel, an isolated 30 GeV muon with $|\eta| < 2.1$ is required to fire the trigger, and an opposite-charge isolated hadronic tau is required with $p_\text{T} > 30\,\text{GeV}$ and $|\eta| < 2.3$. In the $\mu\tau_e$ channel, an isolated 25 GeV muon with $|\eta| < 2.1$ and an isolated electron with $p_\text{T} > 10\,\text{GeV}$ and $|\eta| < 2.3$ are required to fire an electron-muon trigger. Further optimization of the electron, muon, and τ_h kinematic cuts, as well as cuts on angles between the reconstructed objects and p_T^miss, help reduce the background from $W+$ jets.

The background from $Z \to \tau\tau$, which dominates in the $\mu\tau_e$ channel, is estimated from "replacing" muons in $Z \to \mu\mu$ data with taus from simulation. The background from jets faking hadronic taus, which dominates in the $\mu\tau_\text{h}$ channel, is estimated from a data control sample with non-isolated hadronic taus and validated in a control sample where the muon and the tau have the same charge. Finally, the remaining top background is taken from simulation with a normalization factor derived from a b-tagged data sample. The resulting di-tau collinear mass distributions are shown in fig. 5 after fitting for signal and background with a binned maximum likelihood fit. Collinear mass, which is a variable that improves the di-tau mass resolution by utilizing the collinearity of the event p_T^miss with the hadronic tau in real di-tau decays, is explained in more detail in ref. [13]. There is a combined 2.4σ excess, corresponding to a best-fit branching fraction of $BR(H \to \mu\tau) = (0.84^{+0.39}_{-0.37})\%$. If instead the result is interpreted as null, the observed upper limit is 1.51% at 95% CL, which corresponds to a limit on the lepton-flavor-violating Yukawa coupling of 3.6×10^{-3}.

3˙2. *Low-E_T mono-photon search for SUSY Higgs decay.* – In gauge-mediated SUSY breaking (GMSB) models, if the lightest neutralino is light enough, the Higgs can decay via $H \to \tilde{\chi}_1^0\tilde{G}$. The lightest neutralino further decays to a photon and a gravitino $\tilde{G}$.

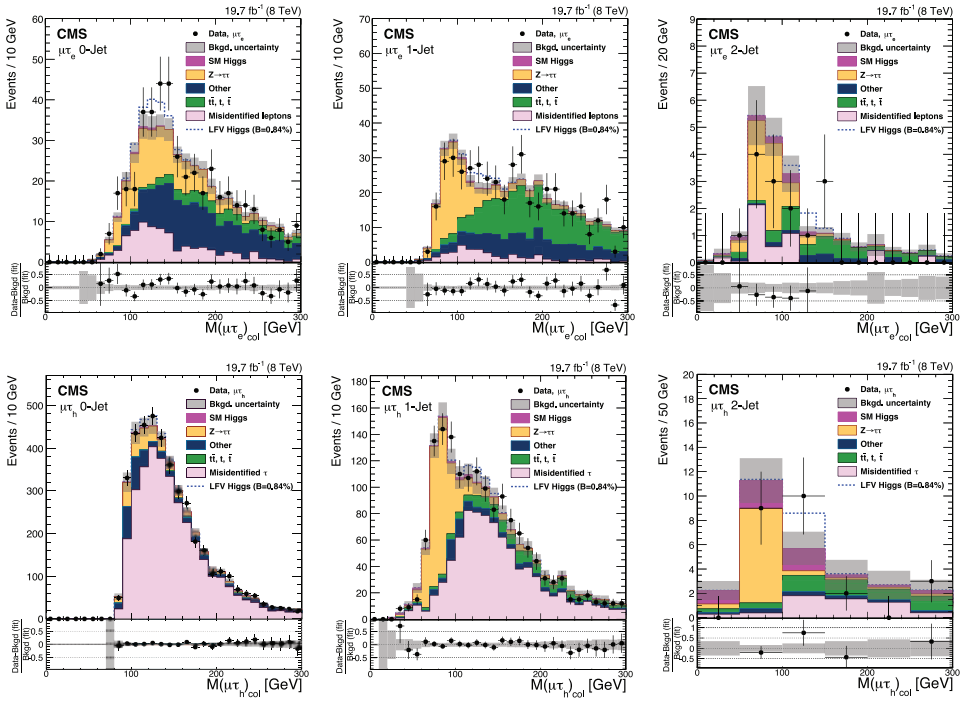

Fig. 5. – Collinear mass distributions after fitting for signal and background, from the $H \to \mu\tau$ search. Top left: $\mu\tau_e$, 0 jets. Top middle: $\mu\tau_e$, 1 jet. Top right: $\mu\tau_e$, 2 jets. Bottom left: $\mu\tau_{\rm h}$, 0 jets. Bottom middle: $\mu\tau_{\rm h}$, 1 jet. Bottom right: $\mu\tau_{\rm h}$, 2 jets.

Both gravitinos leave a signature of $p_{\rm T}^{\rm miss}$ in the detector, and due to the relatively low mass of the neutralino, the decay photon tends to be low in $E_{\rm T}$. The CMS search [14] for this signature relies on pre-scaled data taken with a special low-$E_{\rm T}$, low-$p_{\rm T}^{\rm miss}$ trigger that was not reconstructed until after the end of LHC Run I, so as not to delay processing of high-$E_{\rm T}$ data of more general interest to the collaboration.

In addition to the photon and $p_{\rm T}^{\rm miss}$ requirement, the baseline analysis vetoes on the presence of electrons and muons in the event. One sub-analysis, targeted specifically to $H \to \tilde{\chi}_1^0 \tilde{G}$, makes no jet requirement but cuts on variables that distinguish true $p_{\rm T}^{\rm miss}$ from jet mis-measurement. The other sub-analysis is less model dependent and simply requires ≤ 1 jet and a veto on events where the photon and jet are back to back. As no excess is observed, fig. 6 shows the upper limits derived from both analyses. In particular, the allowed branching ratio for a GMSB decay of the 125 GeV Higgs is $<$ (10–40)%, depending on the neutralino mass.

3˙3. *Heavy $Z\gamma$ resonance.* – Two-Higgs doublet models (2HDM) generically predict extra Higgs scalars and pseudoscalars along with the SM-like 125 GeV Higgs. Production of a heavy pseudoscalar A and subsequent decay to $Z(\to l^+l^-)\gamma$ provides a clean final state with very little SM background. The CMS search for this decay [15] relies on the excellent $ee\gamma$ and $\mu\mu\gamma$ mass resolution of the detector in order to access models with both broad and narrow pseudoscalar resonances. The results of a fit to the $ee\gamma$ and $\mu\mu\gamma$ invariant mass spectra are interpreted as upper limits on the gluon fusion production cross-section of the A times the branching ratio to $ll\gamma$, and are shown in fig. 7.

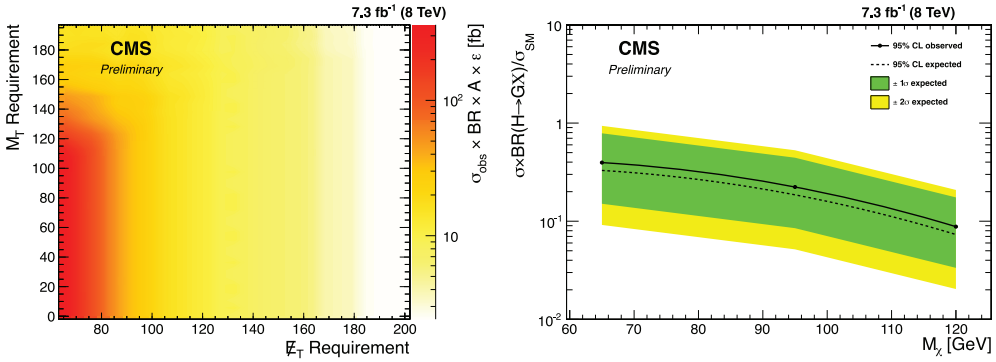

Fig. 6. – Left: observed upper limit on cross-section times branching ratio to photon + $p_{\mathrm{T}}^{\mathrm{miss}}$ times detector acceptance times detector efficiency for the model-independent analysis, for different values of transverse mass (y-axis) and $p_{\mathrm{T}}^{\mathrm{miss}}$ (x-axis) cuts. Right: upper limit on $\sigma \times BR(H \to \tilde{\chi}_1^0 \tilde{G})/\sigma_{\mathrm{SM}}$ as a function of $m_{\tilde{\chi}_1^0}$ for the targeted analysis.

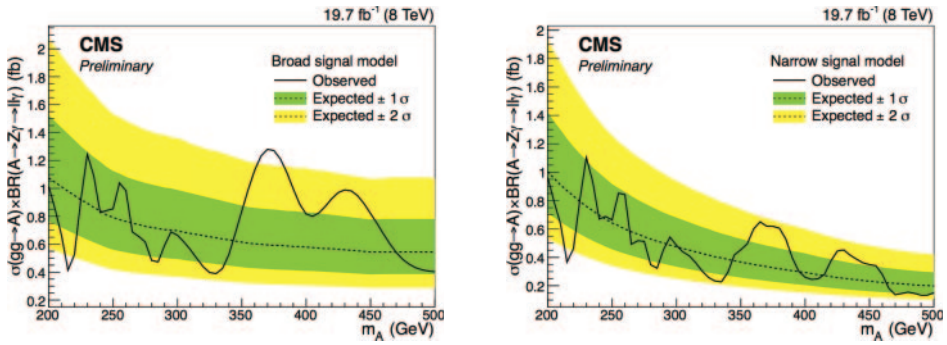

Fig. 7. – Upper limit on the gluon fusion production cross-section of the A times the branching ratio to $ll\gamma$ for a broad A resonance model (left) and a narrow A resonance model (right).

The signal model is a double crystal ball (crystal ball + Gaussian) with SM Higgs width (width equal to 1% of mass) for the broad (narrow) resonances. The observed limit is consistent with the expected limit within the error bands.

3˙4. *Higgs + single top.* – Studies of the top-Higgs coupling C_t can yield important insights into the nature of the Higgs boson. If the Higgs has negative couplings to fermions, the rate of tree-level Higgs production in association with a single top quark can be enhanced 15-fold with respect to the SM expectation. The CMS search for the tHq final state utilizes the WW decay of the Higgs and the leptonic decays of the top, and is divided into two final states: tri-leptons, where both Ws decay leptonically; and same-sign di-leptons, where the lepton from $t \to W(\to l\nu)b$ has the same charge as the one of the Ws from the Higgs decay. Only electron and muon decay modes are considered in the search. b jets from top decay are identified with the CSV algorithm, and forward jets are tagged as well. In the same-sign channel, a multivariate lepton identification discriminator is used in the same-sign analysis to reject jet fakes, hadron decays, and photon conversions. A looser lepton ID is applied in the tri-lepton channel, but the background from $Z \to ll$ is reduced by requiring any di-lepton pair invariant

mass to be off the Z peak and $p_{\mathrm{T}}^{\mathrm{miss}} > 30$ GeV. In both channels, a counting experiment is performed, with the signal region defined by the output of a multivariate likelihood discriminator. In the signal region, the main background comes from fake leptons, either from heavy flavor hadron decays or light jets faking leptons, and is estimated from data. More details about the analysis methods can be found in ref. [16].

No excess of events above the expected background is observed, leading to an interpretation of the results in terms of an upper limit on the process cross-section. The same-sign and tri-lepton analyses are combined to produce an upper limit of 6.7 times the cross-section for $C_t = -1$.

4. – Conclusion

CMS research into SUSY models and exotic Higgs decays remained active and fruitful following the end of LHC Run I. The M_{T2} analysis has probed gluino masses up to almost 1.4 TeV, while the b-tagged razor analysis has probed stop masses up to ~ 600 GeV. The first direct search for $H \to \mu\tau$ yielded a limit on the branching ratio of 1.51%, approximately 10 times more stringent than the previous indirect limit. In addition, important searches have been performed for heavy resonances, multi-lepton final states, mono-photons, and Higgs + single top. Data from LHC Run II will help to clarify some of the observed tensions with the Standard Model and extend the reach into models of physics beyond it.

REFERENCES

[1] Martin S., *Adv. Ser. Direct. High Energy Phys.*, **21** (2010) 1.
[2] ATLAS Collaboration, *Phys. Lett. B*, **716** (2012) 1.
[3] CMS Collaboration, *Phys. Lett. B*, **716** (2012) 30.
[4] CMS Collaboration, *J. Instrum.*, **3** (2008) S08004.
[5] Lester C. and Summers D., *Phys. Lett. B*, **463** (1999) 99.
[6] CMS Collaboration, *JHEP*, **05** (2015) 078, CERN-PH-EP-2015-017, arXiv:1502.04358 [hep-ex].
[7] Rogan C., arXiv:1006.2727 [hep-ph] (2010).
[8] CMS Collaboration, *Phys. Rev. D*, **91** (2015) 52018.
[9] CMS Collaboration, *Phys. Lett. B*, **745** (2015) 5, CERN-PH-EP-2014-286, arXiv: 1412.4109 [hep-ex].
[10] Hinchliffe I., Paige F., Shapiro M., Soderqvist J. and Yao W., *Phys. Rev. D*, **55** (1997) 5520.
[11] CMS Collaboration, *JHEP*, **04** (2015) 124, CERN-PH-EP-2015-033, arXiv:1502.06031 [hep-ex].
[12] CMS Collaboration, *Phys. Lett. B*, **716** (2012) 260.
[13] CMS Collaboration, *Phys. Lett. B*, **749** (2015) 337, CERN-PH-EP-2015-027, arXiv: 1502.07400 [hep-ex].
[14] CMS Collaboration, CMS-PAS-HIG-14-024 (2015).
[15] CMS Collaboration, CMS-PAS-HIG-14-031 (2015).
[16] CMS Collaboration, CMS-PAS-HIG-14-026 (2015).